

Online Research @ Cardiff

This is an Open Access document downloaded from ORCA, Cardiff University's institutional repository: <https://orca.cardiff.ac.uk/id/eprint/119635/>

This is the author's version of a work that was submitted to / accepted for publication.

Citation for final published version:

Glessgen, Carl, Gallichan, Daniel ORCID: <https://orcid.org/0000-0002-0143-2855>, Moor, Manuela, Hainc, Nicola and Federau, Christian 2019. Evaluation of 3D fat-navigator based retrospective motion correction in the clinical setting of patients with brain tumors. *Neuroradiology* 61 (5) , pp. 557-563. 10.1007/s00234-019-02160-w file

Publishers page: <https://doi.org/10.1007/s00234-019-02160-w>
<<https://doi.org/10.1007/s00234-019-02160-w>>

Please note:

Changes made as a result of publishing processes such as copy-editing, formatting and page numbers may not be reflected in this version. For the definitive version of this publication, please refer to the published source. You are advised to consult the publisher's version if you wish to cite this paper.

This version is being made available in accordance with publisher policies.

See

<http://orca.cf.ac.uk/policies.html> for usage policies. Copyright and moral rights for publications made available in ORCA are retained by the copyright holders.



Evaluation of 3D fat-navigator based retrospective motion correction in the clinical setting of patients with brain tumors

Glessgen, Carl¹; Gallichan, Daniel²; Moor, Manuela¹; Hainc, Nicolin^{1,3}; Federau, Christian^{1,4}

Contact: Christian Federau federau@biomed.ee.ethz.ch

1 - Division of Diagnostic and Interventional Neuroradiology, Department of Radiology,
University Hospital Basel, Basel, Switzerland

2 - Cardiff University Brain Research Imaging Centre (CUBRIC), School of Engineering, Cardiff
University, Cardiff, UK

3 - Clinic for Neuroradiology, University Hospital of Zurich, Zurich, Switzerland

4 - Institute for Biomedical Engineering, ETH Zürich and University Zürich,

ABSTRACT

Purpose: A 3D fat-navigator (3D FatNavs) based retrospective motion correction is an elegant approach to correct for motion as it requires no additional hardware and can be acquired during existing 'dead-time' within common 3D protocols. The purpose of this study was to clinically evaluate 3D FatNavs in the work-up of brain tumors.

Materials and Methods: An MRI-based fat-excitation motion navigator incorporated into a standard MPRAGE sequence was acquired in 40 consecutive patients with (or with suspected) brain tumors, pre and post-Gadolinium injection. Each case was categorized into key anatomical landmarks, the temporal lobes, the infra-tentorial region, the basal ganglia, the bifurcations of the middle cerebral artery and the A2 segment of the anterior cerebral artery. First, the severity of motion in the non-corrected MPRAGE was assessed for each landmark, using a 5-point score from 0 (no artifacts) to 4 (non-diagnostic). Second, the improvement in image quality in each pair and for each landmark was assessed blindly using a 4-point score from 0 (identical) to 3 (strong correction).

Results: The mean image improvement score throughout the datasets was 0.54. Uncorrected cases with light and no artifacts displayed scores of 0.50 and 0.13 respectively, while cases with moderate artifacts, severe artifacts and non-diagnostic image quality revealed a mean score of 1.17, 2.25 and 1.38 respectively.

Conclusion: Fat-navigator based retrospective motion correction significantly improved MPRAGE image quality in restless patients during MRI acquisition. There was no loss of image quality in patients with little or no motion, and improvements were consistent in patients who moved more.

INTRODUCTION

A large group of patients, such as patients with dementia, Alzheimer disease, essential tremor or dystonia, Parkinson disease, epilepsy, or confusion can have difficulties staying quiet during a magnetic resonance (MR) imaging scan. Patient motion during MR scans can reduce image quality, weakening the diagnostic value of the examination, leading to repeated imaging, and increasing overall scan time and costs [1].

To cope with this challenge, different motion correction techniques have been developed. Early approaches already included radio frequency (RF)-based tracking systems and prospective motion correction [2, 3]. Recent methods range from external optical tracking systems [4–7] to MR-based motion tracking using self-navigation [8], navigator echoes [9], and image-based motion tracking [10]. Prospective motion correction techniques, such as vNav [11], PROMO [12], PACE [10] and FatNav [13, 14], involving the acquisition of a navigator around the readout train to update the imaging coordinates were successfully employed in the experimental setting, often with healthy volunteers being asked to move on command [11, 12]. Yet to our knowledge, studies on the added value of motion-correction in the clinical setting are sparse [15–17]. Further, many motion correction strategies require additional hardware and can require additional scan-time for additional motion-navigator scans or to repeat the acquisition of motion-corrupted subsets of the main data.

In this context, techniques which can be implemented into dead-time portions of imaging acquisition are better fitted for clinical practice since they allow motion correction without an additional time penalty. The 3D fat-based motion navigator (3D FatNavs) method [18] is one technique, collecting a low-resolution fat image in the dead-time portion of scans to perform retrospective motion correction, and has been demonstrated to correct with high accuracy and produce excellent ultrahigh resolution images at high field strength [19, 20]. Previous works already used the high acceleration factors actionable by fat-selective excitation, to prospectively

correct their datasets using 2D [13] and 3D navigators [14], yet again in a research or phantom-based setting.

The purpose of this study was to retrospectively quantify the added value of motion correction based on a 3D fat-based motion navigator (3D FatNavs) in the clinical setting of routine brain MRI scans.

MATERIALS AND METHODS

1. Study description

This retrospective study was approved by the institutional review board of the __BLINDED FOR REVIEW__. The standard MPAGE of our tumor brain protocol was replaced with a 3D FatNav MPAGE sequence, described in detail below, in 40 consecutive patients with either suspicion of brain tumor, follow-up of tumor recurrence, or immediate post-operative margin controls.

2. Image acquisition

All studies were performed at the clinical facilities of the __BLINDED FOR REVIEW__ using the same 3-T MR imaging device MAGNETOM Skyra 3T (Siemens Healthcare, Erlangen, Germany), fitted with a maximum of 48-channel receiver head coil array. All patients underwent the same imaging protocol, which comprised a native and a contrast-enhanced three-dimensional, T1-weighted, gradient-echo MPAGE, diffusion and susceptibility-weighted imaging, a T2-weighted spin echo sequence, a FLAIR sequence and a perfusion protocol.

When there was no contraindication for intravenous Gadolinium chelate contrast injection, a 3D MPAGE post-Gadolinium sequence was acquired, with each patient imaged receiving gadoterate meglumine (Dotarem, Guerbet, Villepinte, France) at either fixed doses of 20 mL or

weight-based doses of 0.02 mL/Kg. Single adjustments were made with regard to the clinical context.

3. 3D FatNavs MPRAGE sequence

Subsequent analysis was performed solely on the native and contrast-enhanced 3D FatNavs MPRAGE sequence. We integrated a fat-based motion-navigator (3D FatNavs) into our standard MPRAGE sequence [21], which had a nominal resolution of 1.00 x 1.00 x 1.00 mm (matrix size = 256 x 256), a repetition time (TR) = 2300 ms, an echo time (TE) = 2.26 ms and an inversion time (TI) = 900 ms. The 3D FatNavs consisted of a 3D gradient-recalled echo (GRE) sequence with a three-pulse binomial excitation to selectively stimulate at the frequency of fat and was acquired into the dead-time portions occurring after the readout train of the 3D MPRAGE and before the next inversion pulse, requiring an overall increase in scan duration of 3.4 seconds for the parallel imaging calibration prescan. The FatNavs acquisition parameters were: 4 mm isotropic resolution, 44 x 64 x 64 matrix size, TE = 2.19 ms, TR = 4.6 ms, bandwidth = 1950 Hz/pixel, flip angle = 3° and $\frac{3}{4}$ partial Fourier (reconstructed with zero filling) in both phase-encoding directions. Parallel imaging acceleration was 4x4 (GRAPPA) resulting in a total of 442 ms for each individual 3D FatNav.

4. 3D FatNavs MPRAGE post-processing

Reconstructed 3D FatNavs were co-registered using the “realign” tool in SPM (Statistical Parametrical Mapping, version 8) and the resulting estimated motion used to perform retrospective motion-correction separately for the raw k-space data from each RF channel of the respective host sequence, accounting for rotations by using the 3D non-uniform fast Fourier transform algorithm implemented by Jeffrey Fessler’s reconstruction toolbox [22]. The motion parameters were converted into the coordinate space of the MPRAGE acquisition prior to applying the

correction. No additional density compensation was applied to k-space (which might be expected to improve image quality in cases of large motion).

Since the inserted 3D FatNavs were used post-hoc to correct for motion that occurred during the acquisition, each study contained one uncorrected dataset and one matching corrected dataset, resulting in a total of four datasets after native and contrast-enhanced imaging.

5. Motion detection

The intercalated navigator sequences of 3D FatNavs were used to derive the absolute rotational (in degrees) and translational (in mm) motion parameters for each patient, in both native and contrast-enhanced studies. Additionally, the average root-mean-square (RMS) rotation and translation was calculated, with RMS values being expressed in degrees for rotation and in mm for translation. Motion parameters were estimated in reference to the coordinate frame of the scanner (as the 3D FatNavs are acquired at isocenter).

6. Anatomical regions of interest

Native and contrast-enhanced studies were assessed using a total of 5 predefined anatomical regions (**Fig. 1**). In the native studies, three structures were considered: the basal ganglia in the axial plane, the temporal lobes in the coronal plane, and the pons and the cerebellum in the sagittal plane. Post-contrast (when available), the A2-segments of the anterior cerebral artery in the sagittal plane and the M1-bifurcation of the middle cerebral artery in the axial plane were assessed additionally to the first three regions of interest. Combining native and contrast-enhanced datasets, 8 regions of interests were assessed in total.

7. Assessment of image quality and motion correction

Each pair of uncorrected and corrected datasets was randomized by one of the co-authors (C.F.). Images were reviewed blindly by two readers, one general radiologist in residency training (C.G.) and one board-certified neuroradiology fellow (N.H.). The reading software used for this evaluation was 3DSlicer [23].

In a first step, the readers graded each the presence of motion artifacts in the 8 regions of all non-corrected studies using a 5-point motion artifacts (MA) score (0 = no artifacts; 1 = light artifacts; 2 = moderate artifacts; 3 = severe artifacts; 4 = non-diagnostic) and an ensuing consensus reading was performed, resulting in one MA score for each study.

Second, at least two weeks after from the first step, the readers blindly evaluated whether one of the image stacks (corrected versus non-corrected) was of better quality and if yes, designated the images with the highest quality. Further, the scale of the improvement for each of the 8 regions was assessed using a 4-point score for image quality improvement following motion correction (IQIMC, 0 = no difference, 1 = light correction; 2 = moderate correction; 3 = strong correction).

Both readers' scores were subsequently averaged into one unique IQIMC score for each of the 8 regions in each case.

8. Statistical analysis

The IQIMC score was calculated for the total population and within the different MA subgroups. The Bland-Altman methodology was used to evaluate the inter-rater reliability for the assessment of both MA and IQIMC scores [24]. Cohen's Kappa (κ) was calculated to assess the inter-rater reliability in designating the image stacks with the better image quality between corrected and non-corrected [25]. Pearson's correlation coefficient was used to evaluate the linear correlation between the various variables. Paired, two-tailed Student t-tests were used to test for statistical significance. The significance level in this study was set to $\alpha = 0.05$

RESULTS

1. *Demographics*

40 patients were included in our study (25 men and 15 women [mean age, 59 years; range, 27-86 years]), with a total of 77 datasets acquired (3 patients did not qualify for contrast-enhanced imaging), yielding a total of 305 anatomical regions to be evaluated for image quality improvement. The mean injected volume of gadoterate meglumine was 17 ± 3.5 mL [range 10-20 mL].

2. *Image quality and quantitative motion detection*

118 regions presented with no motion artifacts (38.7%), 117 with light artifacts (38.4%), 44 with moderate artifacts (14.4%), 6 with severe artifacts (1.97%) and 20 had a non-diagnostic value (6.56%). Nearly all sample values of the Bland-Altman plot for the inter-rater reliability in assessing MA scores were contained within the limits of agreement, with a mean bias of -0.04 between the two readers, **Fig.2**.

The average RMS rotation and translation values during the scan for the native and contrast-enhanced datasets were of 0.54° and 0.52 mm and 0.33° and 0.40 mm, respectively. Contrast-enhanced datasets displayed significantly lower average RMS rotation and translation values ($p < 0.001$).

The average RMS rotation and translation values showed a positive, significant correlation with the MA scores achieved, 0.31 and 0.50 respectively ($p < 0.001$), **Fig.3**.

3. *Image quality improvement after motion correction*

The overall average IQIMC score was 0.54 ± 0.06 . With regard to MA subgroups, IQIMC scores were 0.13 ± 0.36 for the regions without artifacts, 0.50 ± 0.59 for the regions with light artifacts, 1.17 ± 0.64 for the regions with moderate artifacts, 2.25 ± 0.61 for the regions with severe

artifacts and 1.38 ± 1.04 for the non-diagnostic regions. None (0/305) of the corrected anatomical regions was assessed as inferior in image quality by comparison with its non-corrected match.

Inter-rater reliability for the blind designation of the image with highest quality was strong ($\kappa=0.862$, $p < 0.001$). Nearly all sample values of the Bland-Altman plot for the inter-rater reliability in assessing MC scores were contained within the limits of agreement, with a mean bias of -0.19 between the two readers, Fig.2.

Average RMS rotation and translation values, as well as the MA scores showed a positive, significant correlation with the IQIMC scores achieved, 0.55, 0.61 and 0.62 respectively ($p<0.001$), Fig.3. Examples of the typical image quality improvement obtained after utilization of 3D FatNavs are shown in Fig.4.

DISCUSSION

This study shows that 3D FatNavs with retrospective motion correction significantly improves image quality in patients with light to strong head motion during the scan, without altering the quality of images in patients with non-relevant motion, and with a negligible effect on overall scan time. Moderately and severely impaired regions displayed the highest motion correction values. Importantly, none of the of 305 anatomical regions evaluated showed image quality decrease after application of the retrospective correction.

Very few studies report the use of motion correction techniques for head imaging in a clinical setting. Prospective motion correction in high-resolution 3D-T2-FLAIR acquisitions has been shown to be of interest [17] in epilepsy patients, however with several limitations, such as additional scan duration if the acquired stack was considered impaired. This study also lacked intraindividual assessment of motion correction between scans with and without the motion correction. Kochunov et al. [15] reported a retrospective motion correction technique using repetitive scanning and subsequent averaging of image stacks, with conclusive results but a requiring a significant increase of total scan duration.

Compared to prospective motion correction techniques, retrospective motion correction method has in the clinical setting the advantage that non-corrected images are still acquired and available, which might increase the acceptance of the method in the workflow.

In our study, the observed image improvement following motion correction significantly increased with the extent of the patients' motion. This underlines the better performance of the correction tool given a more impaired dataset, while no or minimal motion could not be improved in a way to be subjectively noticeable.

Interestingly, despite the correlation between the motion artifact scores and average RMS motion parameters, some patients with limited measured motion during the scan presented with

larger-scaled motion artifacts. This might be due to the fact that cumulative effects of small rotations and translations might be responsible for larger motion artifacts.

It is also possible that part of this motion was not detected by the navigator, and therefore could not be corrected. These cases do not account for a majority, however, since inter-scan motion represented the greater part of the overall head motion. As expected, even the 3D FatNavs motion correction could not produce high-quality images in the most severe cases of motion.

Finally, given the posterior rotational center of the head, and the rigid body correction approach, the readers did not notice a higher occurrence of motion artifacts for the anterior areas, or for the infratentorial region. Average motion scores for the respective regions stayed within a similar, fit-to-comparison range, so that no further analyses were performed. Further, by breaking down our overall sample to each landmark, statistical power would have been compromised.

The benefit of 3D FatNavs in terms of motion correction can certainly be extrapolated to other sequences than the MPRAGE, as well as other patient groups, although the technique is currently only employable for 3D sequences. For other acquisition schemes than MPRAGE, the scan time might be slightly increased, depending on the available dead-time within the particular sequence.

Certain limitations have to be acknowledged for this study. First, this was a single center retrospective study, without patient randomization or control for clinical factors. The number of patients was relatively small (nonetheless a larger cohort than most of the previous related studies). The average RMS motion parameters were not identical when compared intra-individually, with significantly lower values for contrast-enhanced studies compared to pre-contrast. We suspect that this results from the fact that patients were better accustomed to the MRI environment after one acquisition series, with gradual acclimation [26].

In conclusion, this study shows that motion correction using 3D FatNavs successfully and reliably corrects for rigid head motion in the setting of clinical brain MRI studies, with negligible effect on total scan time.

We declare that we have no conflict of interest.

REFERENCES

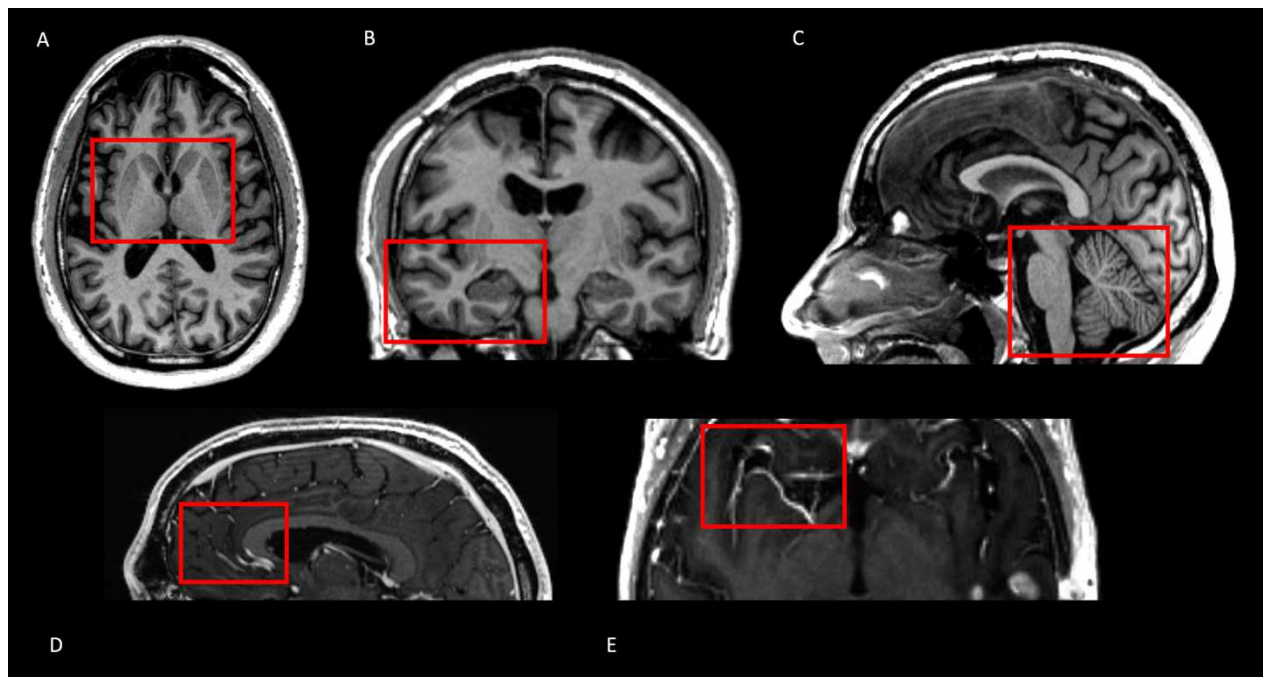
1. Andre JB, Bresnahan BW, Mossa-Basha M, et al (2015) Toward Quantifying the Prevalence, Severity, and Cost Associated With Patient Motion During Clinical MR Examinations. *J Am Coll Radiol* 12:689–695
2. Haacke EM, Patrick JL (1986) Reducing motion artifacts in two-dimensional Fourier transform imaging. *Magn Reson Imaging* 4:359–76
3. Ackerman J (1986) Rapid 3D tracking of small RF coils. In: *Proc 5th Annual Meeting of ISMRM*. Montréal, Canada, pp 1131–2
4. Zaitsev M, Dold C, Sakas G, et al (2006) Magnetic resonance imaging of freely moving objects: prospective real-time motion correction using an external optical motion tracking system. *Neuroimage* 31:1038–1050
5. Qin L, van Gelderen P, Derbyshire JA, et al (2009) Prospective head-movement correction for high-resolution MRI using an in-bore optical tracking system. *Magn Reson Med* 62:924–934
6. Schulz J, Siegert T, Reimer E, et al (2012) An embedded optical tracking system for motion-corrected magnetic resonance imaging at 7T. *Magn Reson Mater Physics, Biol Med* 25:443–453
7. Maclaren J, Armstrong BSR, Barrows RT, et al (2012) Measurement and Correction of Microscopic Head Motion during Magnetic Resonance Imaging of the Brain. *PLoS One* 7:e48088
8. Pipe JG (1999) Motion correction with PROPELLER MRI: application to head motion and free-breathing cardiac imaging. *Magn Reson Med* 42:963–9
9. Lin W, Huang F, Börnert P, et al (2010) Motion correction using an enhanced floating navigator and GRAPPA operations. *Magn Reson Med* 63:339–348

10. Thesen S, Heid O, Mueller E, Schad LR (2000) Prospective acquisition correction for head motion with image-based tracking for real-time fMRI. *Magn Reson Med* 44:457–65
11. Tisdall MD, Hess AT, Reuter M, et al (2012) Volumetric navigators for prospective motion correction and selective reacquisition in neuroanatomical MRI. *Magn Reson Med* 68:389–399
12. White N, Roddey C, Shankaranarayanan A, et al (2010) PROMO: Real-time prospective motion correction in MRI using image-based tracking. *Magn Reson Med* 63:91–105
13. Skare S, Hartwig A, Mårtensson M, et al (2015) Properties of a 2D fat navigator for prospective image domain correction of nodding motion in brain MRI. *Magn Reson Med* 73:1110–1119
14. Engström M, Mårtensson M, Avventi E, et al (2015) Collapsed fat navigators for brain 3D rigid body motion. *Magn Reson Imaging* 33:984–991
15. Kochunov P, Lancaster JL, Glahn DC, et al (2006) Retrospective motion correction protocol for high-resolution anatomical MRI. *Hum Brain Mapp* 27:957–962
16. Brown TT, Kuperman JM, Erhart M, et al (2010) Prospective motion correction of high-resolution magnetic resonance imaging data in children. *Neuroimage* 53:139–145
17. Vos SB, Micallef C, Barkhof F, et al (2018) Evaluation of prospective motion correction of high-resolution 3D-T2-FLAIR acquisitions in epilepsy patients. *J Neuroradiol.*
18. Gallichan D, Marques JP, Gruetter R (2016) Retrospective correction of involuntary microscopic head movement using highly accelerated fat image navigators (3D FatNavs) at 7T. *Magn Reson Med* 75:1030–1039
19. Federau C, Gallichan D (2016) Motion-Correction Enabled Ultra-High Resolution In-Vivo 7T-MRI of the Brain. *PLoS One* 11:e0154974
20. Lüsebrink F, Sciarra A, Mattern H, et al (2017) T1-weighted in vivo human whole brain MRI dataset with an ultrahigh isotropic resolution of 250 μm . *Sci Data* 4:170032
21. Brant-Zawadzki M, Gillan GD, Nitz WR (1992) MP RAGE: a three-dimensional, T1-

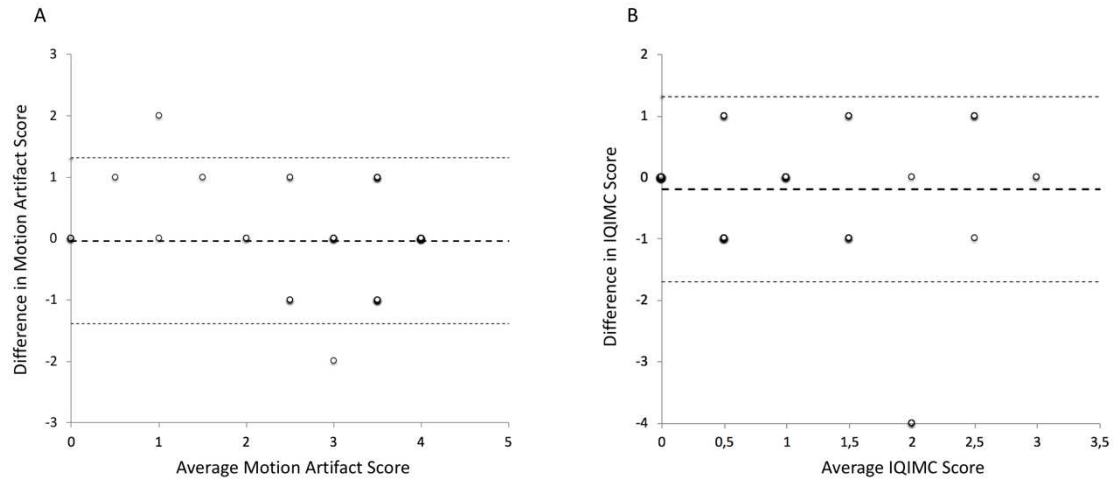
weighted, gradient-echo sequence--initial experience in the brain. *Radiology* 182:769–75

22. Fessler JA Michigan Image Reconstruction Toolbox.
<http://web.eecs.umich.edu/~fessler/code/>. Accessed 1 Aug 2018
23. SlicerCommunity 3DSlicer. <https://www.slicer.org>. Accessed 5 Jul 2018
24. Bland JM, Altman DG (1986) Statistical methods for assessing agreement between two methods of clinical measurement. *Lancet* (London, England) 1:307–10
25. McHugh ML (2012) Interrater reliability: the kappa statistic. *Biochem medica* 22:276–82
26. van Minde D, Klaming L, Weda H (2013) Pinpointing Moments of High Anxiety During an MRI Examination. *Int J Behav Med* 21:487–95

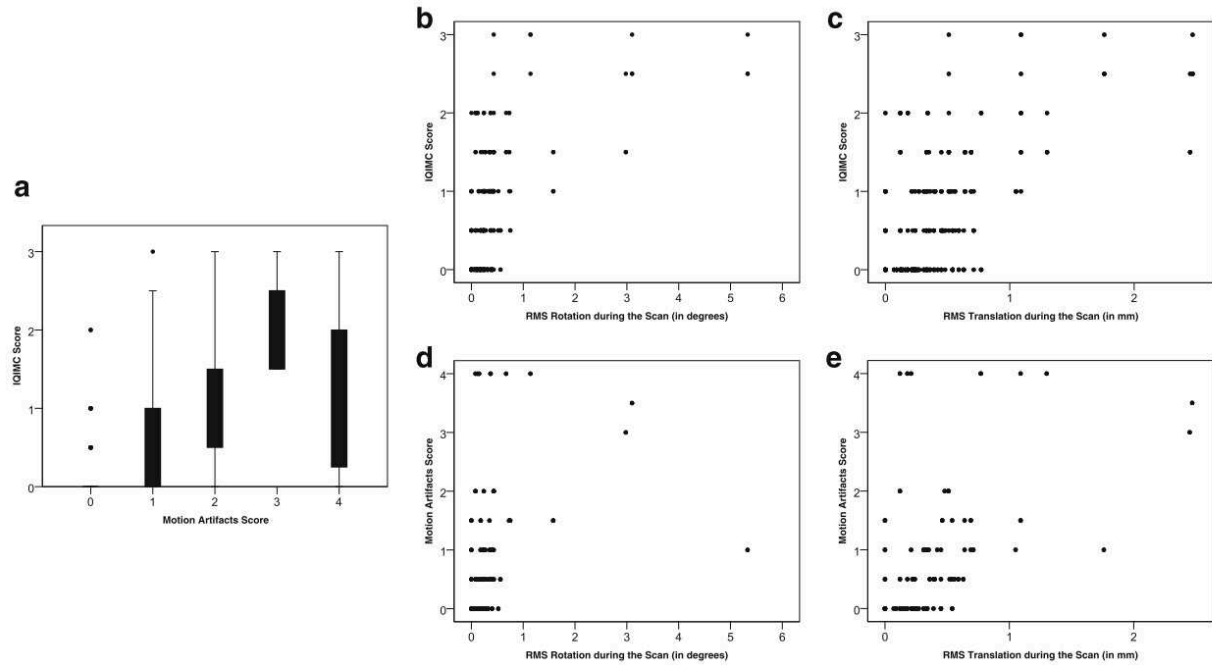
Figures



1. Planes and anatomical landmarks used for the assessment of artifacts and motion correction. A. Axial plane, view of the basal ganglia. B. Coronal plane, view of the temporal lobes. C. Sagittal plane, view of the infratentorial region. D. Sagittal plane, A2 segments of the anterior cerebral arteries. E. Axial plane, view of the M1 segment of the medial cerebral artery.

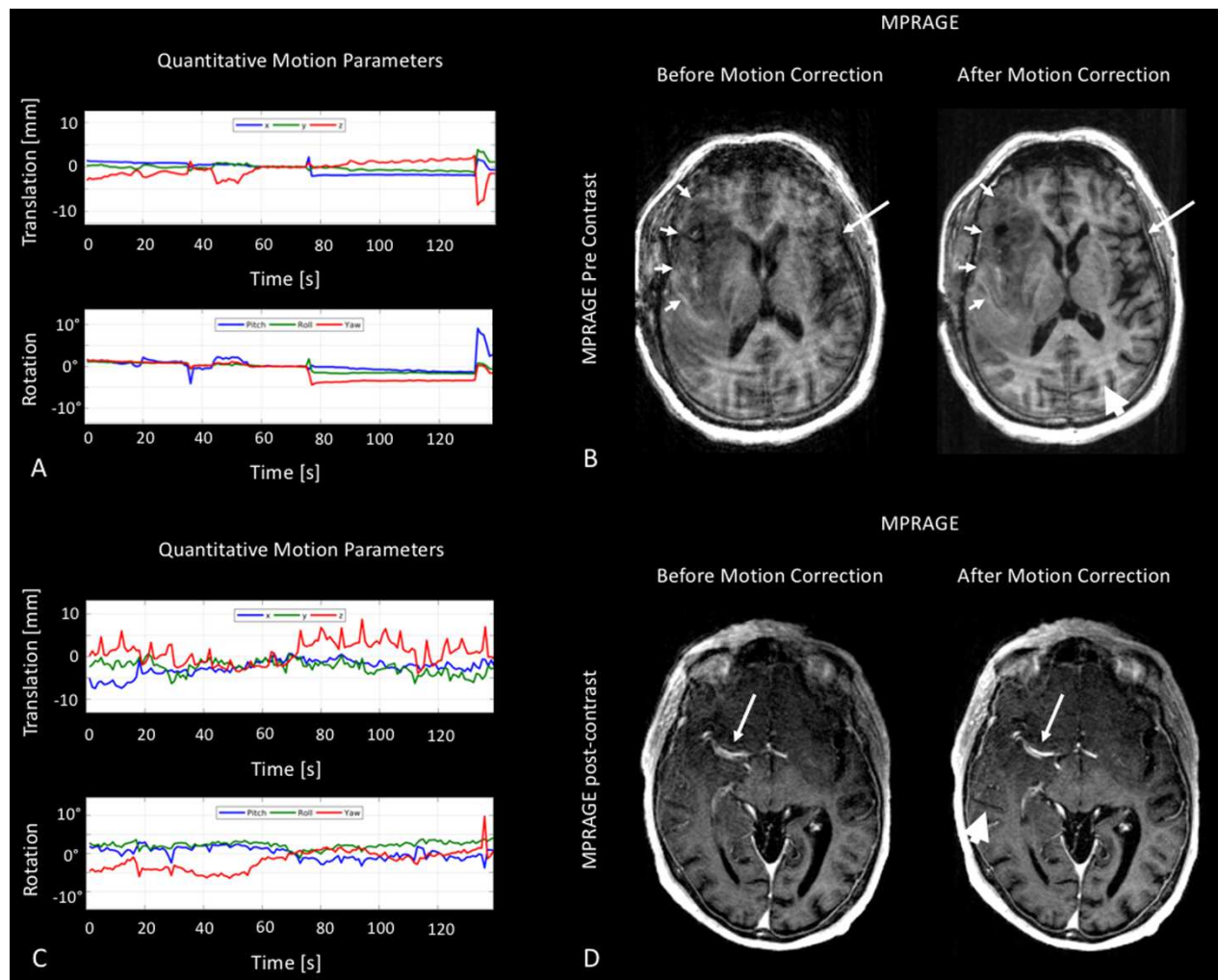


2. Bland-Altman plots for the evaluation of the inter-rater reliability in assessing the Motion Artifacts scores (A) and the IQIMC scores (B). Only single values are situated outside the limits of agreements (small dotted lines) and most values are gathered around the mean score difference (bold dotted line).



3. A. Box plot of the IQIMC scores in relation to the Motion Artifacts scores of the uncorrected datasets.

The value of the correction is increasing with the severity of the motion, up to the worst images, in which a correction was not always possible. B-E. Scatter graphs of the IQIMC and MA scores in relation to the average RMS rotation and translation values. Note the increasing IQIMC scores as the body motion increases. MA scores display a partial correlation with the RMS motion values, probably due to the combination of rotation and translation in patients with high MA scores.



4. A-B. Postoperative control after partial resection of a glioblastoma multiforme in a 48-year-old man. The patient presented with large, bulk motion during the scan, both translational (RMS 2.47mm) and rotational (RMS 3.10°). The remaining tumor fronto-temporo-insular right (small white arrows), can be better delineated after motion correction. The left frontal operculum (long white arrow) particularly benefited from the motion correction. Although the images' clearness and overall quality significantly improved after motion correction, residual motion artifacts nevertheless remained (white large arrowhead). C-D. Control in the course of a Temodal therapy in a 70 year old woman with known glioblastoma multiforme. Rigid body motion for this patient was limited, with smaller values of translational (RMS 0.51 mm) and rotational (RMS 0.43°) motion than the previous case. The M1 segment of the right medial cerebral artery displays sharper margins (long arrow), as well as the sulcus temporalis inferior on the right side (arrowhead).